Energy Bands of PbTe, PbSe, and PbS†

PAY JUNE LIN*
Institute for the Study of Metals, University of Chicago, Chicago, Illinois

AND

LEONARD KLEINMAN‡
Department of Physics, University of Southern California, Los Angeles, California

(Received 12 August 1965)

Because it is impossible to obtain first-principle crystal potentials of the lead salts with sufficient accuracy to calculate energy bands in agreement with experiment, we have developed a new pseudopotential containing only $2n+1$ adjustable parameters, where n is the number of different atoms per unit cell. This pseudopotential contains all the important relativistic effects including spin-orbit interactions and yet requires only 5 parameters for the lead salts. We have chosen the parameters to fit the ordering of the six levels around the forbidden energy gap at the $(\frac{111}{222})$ point on the Brillouin-zone face as well as two optically measured energy gaps presumed to be at the center of the zone. The energy bands obtained are in very good agreement with the rest of the optical data, the photoelectric data, and the pressure dependence of the forbidden gap. Reasonably good agreement is obtained between our calculated effective masses and g values and the experimentally determined ones.

I. INTRODUCTION

THE lead salts, PbTe, PbSe, and PbS are partially polar semiconductors with an average valence of five and crystalize in the rock salt structure. Their known characteristics such as small energy gaps, low resistivities, large carrier mobilities, and unusually high dielectric constants which do not usually appear in polar crystals, have made the various electrical and optical measurements possible, thus allowing a close view of the relationship between the optical, electrical, and chemical properties of polar crystals. So far the investigation of these materials has been focused on the transport properties and the electronic structures. Cyclotron resonance[1] yields reliable values for effective masses and their anisotropy. Magneto-optical transitions[2–6] provide information about the structure near the band extrema. De Haas–van Alphen oscillatory magnetic susceptibility,[7] Shubnikov–de Haas oscillatory magnetoresistance,[8–12] piezoresistance,[13–15] and other optical and transport phenomena,[16–24] have all been observed extensively. The knowledge amassed

† This research was begun when both authors were at the University of Pennsylvania and was supported by the Advanced Research Projects Agency.

* Supported by the National Science Foundation and the U. S. Office of Naval Research.

‡ Supported by Joint Services Electronics Program (U. S. Army, U. S. Navy, and U. S. Air Force) under Grant No. AF-AFOSR-496-65.

[1] P. J. Stiles, E. Burstein, and D. N. Langenberg, in *Proceedings of the International Conference on the Physics of Semiconductors, Exeter, 1962* (The Institute of Physics and The Physical Society, London, 1962), p. 577.

[2] E. D. Palik, D. L. Mitchell, and J. N. Zemel, Phys. Rev. **135**, A763 (1964).

[3] D. L. Mitchell, E. D. Palik, and J. N. Zemel, in *Proceedings of the International Conference on the Physics of Semiconductors, Paris, 1964* (Academic Press Inc., New York, 1965), p. 325.

[4] E. D. Palik, S. Teitler, B. W. Henvis, and R. F. Wallis, in *Proceedings of the International Conference on the Physics of Semiconductors, Exeter, 1962* (The Institute of Physics and The Physical Society, London, 1962), p. 288.

[5] E. D. Palik and D. L. Mitchell, Bull. Am. Phys. Soc. **9**, 292 (1964); and D. L. Mitchell, E. D. Palik, J. D. Jensen, R. B. Schoolar, and J. N. Zemel, *ibid.* **9**, 292 (1964).

[6] D. L. Mitchell, E. D. Palik, J. D. Jensen, R. B. Schoolar, and J. N. Zemel, Phys. Letters **4**, 262 (1963).

[7] P. J. Stiles, E. Burstein, and D. N. Langenberg, J. Appl. Phys. Suppl. **32**, 2174 (1961).

[8] K. F. Cuff, M. R. Ellett, and C. D. Kuglin, in *Proceedings of the International Conference on the Physics of Semiconductors, Exeter, 1962* (The Institute of Physics and The Physical Society, London, 1962), p. 316.

[9] K. F. Cuff, M. R. Ellett, and C. D. Kuglin, J. Appl. Phys. Suppl. **32**, 2179 (1961).

[10] R. S. Allgaier, Phys. Rev. **119**, 554 (1960).

[11] R. S. Allgaier, B. B. Houston, and J. R. Burke, Bull. Am. Phys. Soc. **8**, 517 (1963).

[12] K. F. Cuff, M. R. Ellet, C. D. Kuglin, and L. R. Williams, in *Proceedings of the International Conference on the Physics of Semiconductors, Paris, 1964* (Academic Press Inc., New York, 1965), p. 677.

[13] Y. V. Ilisavskii and E. Z. Yakhkind, Fiz. Tverd. Tela **4**, 1975 (1962) [English transl.: Soviet Phys.—Solid State **4**, 1447 (1963)].

[14] Y. V. Ilisavskii, Fiz. Tverd. Tela **4**, 918 (1962) [English transl.: Soviet Phys.—Solid State **4**, 674 (1962)].

[15] A. A. Averkin, U. V. Ilisavsky, and A. R. Regel, in *Proceedings of the International Conference on the Physics of Semiconductors, Exeter, 1962* (The Institute of Physics and The Physical Society, London, 1962), p. 690.

[16] R. Nii, J. Phys. Soc. Japan, **18**, 456 (1963); **19**, 58 (1964).

[17] Y. Kanai, R. Nii, and N. Watanabe, J. Appl. Phys. Suppl. **32**, 2146 (1961).

[18] R. S. Allgaier, J. Appl. Phys. Suppl. **32**, 2185 (1961).

[19] J. R. Dixon and H. R. Riedl, *Proceedings of the International Conference on the Physics of Semiconductors, Exeter, 1962* (The Institute of Physics and The Physical Society, London, 1962), p. 179.

[20] R. S. Allgaier and B. B. Houston, Jr., *Proceedings of the International Conference on the Physics of Semiconductors, Exeter, 1962* (The Institute of Physics and The Physical Society, London, 1962), p. 172.

[21] A. K. Walton, T. S. Moss, and B. Ellis, Proc. Phys. Soc. (London) **79**, 1065 (1962).

[22] W. Paul, M. Demeis, and L. X. Finegold, *Proceedings of the International Conference on the Physics of Semiconductors, Exeter, 1962* (The Institute of Physics and The Physical Society, London, 1962), p. 712.

[23] A. A. Averkin, I. G. Dombrovskaya, and B. Ya. Moizhes, Fiz. Tverd. Tela **5**, 96 (1963) [English transl.: Soviet Phys.—Solid State **5**, 66 (1963)].

[24] M. Cardona and D. L. Greenaway, Phys. Rev. **113**, A1685 (1964).

from these studies is almost conclusive in identifying the location of both the conduction- and valence-band extrema as at the point $L=(\pi/a)(1,1,1)$, on the Brillouin-zone face. The fact that these three semiconductors all have positive temperature coefficients for the forbidden gaps and small effective-mass components leads us to believe that there exists an over-all similarity in their energy-band structures. The only important difference is that the mass anisotropy for PbTe, being about 8-14, is larger than that of PbSe and PbS by approximately an order of magnitude. Therefore the constant energy surfaces for PbTe are prolate ellipsoids of revolution at L while those for PbSe and PbS are nearly spherical.

Here we need a theoretical treatment. However, a calculation from first principles is not practical because of difficulty in obtaining a crystal potential with an accuracy commensurate with the small band gaps. This inaccuracy is attributed to the uncertainties in the approximations used in the calculation of the covalently bonding valence electron contribution to the exchange and correlation potentials. As has been pointed out by Phillips,[25] the s levels are especially sensitive to such small errors in the crystal potentials. The computational difficulties in making the potential self-consistent, and the complexity of the core potential, which, in heavy atoms, involves both a large relativistic effect and the spin-orbit interaction,[26,27] also increase the difficulty of a first principles approach. As an example, Conklin *et al.*[28] have done a nonself-consistent but otherwise first principles relativistic calculation of PbTe. They got remarkably good results; the top of the valence and bottom of the conduction bands had a relative error of only 0.3 eV—but this was enough to interchange the two bands.

The purpose of this work is to devise a new pseudopotential scheme which is capable of producing reasonably good numerical results for solids composed of atoms of high atomic number without going into much more elaborate procedures. We are aiming for a rather general application. In particular, we have worked out the cases of the lead salts.

Our treatment includes all the important relativistic effects and spin-orbit interactions, yet requires only a few adjustable parameters. An advantage of this method is that the band structure can be described more clearly from the presently available experimental data. Some of the experimental data are essential in the calculation while the rest are used to check the consistency of the results.

In the next section we construct a pseudopotential which, because of its physical nature, requires only two arbitrary parameters per atom plus a spin-orbit parameter, a total of five parameters for the lead salts. In the third section we give the formulas for calculating effective masses and g factors. In the last section we show how to choose numerical values for the parameters in our pseudopotential and display the energy bands calculated therefrom. We compare our energy bands with the optical-reflectivity measurements of Cardona and Greenaway and with the photoemission studies of Spicer. Calculated effective masses and g values are compared with experiment and other details of the bands are discussed and compared with experiment.

II. PSEUDOPOTENTIAL

Let us examine several theoretical aspects of the problem before presenting our pseudopotential model. Since the orthogonalized-plane-wave method[29] has been considered the most successful among the existing band calculation methods in getting valence wave functions, we chose to express our crystal valence wave functions in the same manner.

Let $\psi_k{}^\alpha$ be the crystal wave function which transforms according to the irreducible representation Γ_α of the cubic point group. Since $\psi_k{}^\alpha$ should be orthogonal to the atomic core functions $\chi_t{}^\alpha$ of similar symmetry, it can be separated into a smooth part and a core part as expressed in the following form:

$$\psi_k{}^\alpha=\varphi_k{}^\alpha-\sum_t(\varphi_k{}^\alpha,\Phi_{k,t}{}^\alpha)\Phi_{k,t}{}^\alpha, \tag{1}$$

where

$$\Phi_{k,t}{}^\alpha=(1/N)^{1/2}[\sum_{l_1}(\exp i\mathbf{k}\cdot\mathbf{r}_{l_1})\chi_t{}^{\mathrm{Pb}}(\mathbf{r}-\mathbf{r}_{l_1}) +\sum_{l_2}(\exp i\mathbf{k}\cdot\mathbf{r}_{l_2})\chi_t{}^{\mathrm{VI}}(\mathbf{r}-\mathbf{r}_{l_2})]. \tag{2}$$

Here $\mathbf{r}_l$ is the lattice vector, N is the number of unit cells in the crystal, and $\chi_t{}^{\mathrm{Pb}}$, $\chi_t{}^{\mathrm{VI}}$ refer to the core functions corresponding to the two different atoms in the unit cell of the NaCl crystal structure.

The smooth part $\varphi_k{}^\alpha$ may be expanded in a series of symmetrized plane waves transforming like Γ_α, viz.,

$$\varphi_k{}^\alpha=\sum_i a_i(\sum_j C_{ij}{}^\alpha e^{i(\mathbf{k}+\mathbf{K}_{ij})\cdot\mathbf{r}})\equiv\sum_i a_i|K_i{}^\alpha\rangle, \tag{3}$$

where $\mathbf{K}_{ij}$ are reciprocal lattice vectors. The set of vectors $\mathbf{k}+\mathbf{K}_{ij}$ in the bracket, for the same $\mathbf{k}$, and i, all have the same magnitude and are related to each other by operations of the small group of $\mathbf{k}$.

The Schrödinger equation is written as

$$(T+V+H_{\mathrm{so}})\psi_k{}^\alpha=(E+E_{\mathrm{so}})\psi_k{}^\alpha, \tag{4}$$

where T and V denote the kinetic and periodic potential energy, respectively; and H_{so} represents the spin-orbit interaction Hamiltonian.

By substituting Eq. (1) into Eq. (4), we obtain the following equation satisfied by the smooth-part wave function $\varphi_k{}^\alpha$,

$$(T+V+V_R+H_{\mathrm{so}}+V_{\mathrm{so}})\varphi_k{}^\alpha=(E+E_{\mathrm{so}})\varphi_k{}^\alpha, \tag{5}$$

[25] J. C. Phillips, Phys. Rev. **125**, 1931 (1962).
[26] L. E. Johnson, J. B. Conklin, Jr., and G. W. Pratt, Jr., Phys. Rev. Letters **11**, 538 (1963).
[27] F. Herman, C. D. Kuglin, K. F. Cuff, and R. L. Kortum, Phys. Rev. Letters **11**, 541 (1963).
[28] J. B. Conklin, Jr., L. E. Johnson, and G. W. Pratt, Jr., Phys. Rev. **137**, A1282 (1965).
[29] C. Herring, Phys. Rev. **57**, 1169 (1940).

TABLE I. Numerical values of quantities appearing in the pseudopotentials. (The r_0's and β's are taken from atomic wave functions while the Z's and α's are adjustabel parameters chosen to fit the experimental data.)

	PbTe	PbSe	PbS
r_0^{Pb}	$0.493a_0$	$0.493a_0$	$0.493a_0$
r_0^{VI}	$0.412a_0$	$0.264a_0$	$0.169a_0$
β^{Pb}	$3.228a_0^{-1}$	$3.228a_0^{-1}$	$3.228a_0^{-1}$
β^{VI}	$3.597a_0^{-1}$	$4.608a_0^{-1}$	$4.167a_0^{-1}$
Z_{Pb}	2.9	2.9	2.9
Z_{VI}	3.2	3.2	3.2
α_{Pb}	0.125	0.125	0.094
α_{VI}	0.17	0.33	0.366
α	0.78	0.78	0.78

where

$$V_R=\sum_t \frac{-(\varphi_k{}^\alpha,\Phi_{kt}{}^\alpha)[(\Phi_{kt}{}^\alpha|H|\Phi_{kt}{}^\alpha)-E]\Phi_{kt}{}^\alpha}{\varphi_k{}^\alpha} \quad (6)$$

and

$$V_{\mathrm{so}}=\sum_t \frac{-(\varphi_k{}^\alpha,\Phi_{kt}{}^\alpha)[(\Phi_{kt}{}^\alpha|H_{\mathrm{so}}|\Phi_{kt}{}^\alpha)-E_{\mathrm{so}}]\Phi_{kt}{}^\alpha}{\varphi_k{}^\alpha}. \quad (7)$$

The physical significance of the orthogonality of $\psi_k{}^\alpha$ to $\Phi_{kt}{}^\alpha$ can be seen from Eq. (5). This equation shows that the effect of orthogonalization may be accounted for by including a repulsive potential V_R in the valence Hamiltonian. Therefore, $V+V_R$ forms an effective potential for the new Hamiltonian. The eigenvalues of the new Hamiltonian are identical with those of the old one but the eigenfunctions are "smooth" in the sense that they are not oscillatory in the core region.

Phillips and Kleinman[30] have observed the cancellation of V and V_R in the calculation of the Fourier coefficients. Cohen and Heine[31] further demonstrated the details of the cancellation much more explicitly in real space. They showed that within an error of ten percent, the repulsive potential could be expanded in the occupied core states. As the core states form a nearly complete set of functions in the core region, the cancellation of the total potential $V+V_R$ is almost complete inside but nonexistent outside the core, i.e.,

$$V+V_R\approx V(r')[\delta(r-r')-\textstyle\sum_t \chi_t{}^*(r')\chi_t(r)] \quad (8)$$
$$\approx 0 \text{ inside the core.}$$

Based on the preceding arguments, we are now ready to set up a new pseudopotential scheme of calculation. Let us first consider only part of the Hamiltonian, excluding the spin-orbit term for the moment.

The crystal pseudopotential is taken to be a superposition of simple pseudopotentials of the individual atoms. These atomic pseudopotentials can be expressed in the following form:

$$V_{\mathrm{eff}}=0, \qquad r<r_0,$$
$$V_{\mathrm{eff}}=(2Z/r)(1-e^{-\beta(r-r_0)}), \qquad r\geq r_0. \quad (9)$$

[30] J. C. Phillips and L. Kleinman, Phys. Rev. **116**, 287 (1959).
[31] M. H. Cohen and V. Heine, Phys. Rev. **122**, 1821 (1961).

The Fourier transform of V_{eff} is

$$V(K)=\frac{32\pi Z}{Ka^3}\left[-\frac{\cos Kr_0}{K}+\frac{(\beta\sin Kr_0+K\cos Kr_0)}{\beta^2+K^2}\right], \quad (10)$$

where a is the lattice constant. We determine r_0 and β from Slater's[32] analytical atomic wave functions

$$\chi_{5p}{}^{\mathrm{Pb}}=381.8r^3e^{-6.088r},$$
$$\chi_{4p}{}^{\mathrm{Te}}=461.3r^{2.7}e^{-6.554r},$$
$$\chi_{3p}{}^{\mathrm{Se}}=506.4r^2e^{-7.583r}, \quad (11)$$
$$\chi_{2p}{}^{\mathrm{S}}=98.67re^{-5.925r},$$

r_0 and β satisfying the following relations:

$$\chi(r_0)=\mathrm{Max}[\chi(r)]$$

and

$$\beta=(1/r_1-r_2),$$

where r_1, r_2 in turn satisfy the following relations:

$$\chi(r_1)=(\chi(r_0)/2e),$$
$$\chi(r_2)=(\chi(r_0)/2),$$

where $\chi(r)$ is the outermost p core orbital of the atom. This prescription, though not unique, fixes r_0 and β leaving us with only one adjustable parameter per atom, Z.

For lead salts with the NaCl crystal structure, the total contribution from the two different atoms in a unit cell to the Fourier transform is given by

$$V(K)=V^{\mathrm{Pb}}(K)+V^{\mathrm{VI}}(K)\cos(\mathbf{K}\cdot\boldsymbol{\tau})$$
$$=V^{\mathrm{Pb}}(K)\pm V^{\mathrm{VI}}(K), \quad (12)$$

where VI refers to one of the atoms Te, Se, and S, and $\boldsymbol{\tau}=\frac{1}{2}a(1,1,1)$; the plus (minus) sign holds for even (odd) reciprocal lattice vectors $\mathbf{K}$.

In Table I, we have listed the values of r_0, β, and Z which we used for each atom, and in Table II, some Fourier transforms of the pseudopotentials for PbTe, PbSe, and PbS.

To determine the eigenvalues and the coefficients appearing in the expansion of the eigenfunction $\varphi_k{}^\alpha$ in Eq. (3) we only need to diagonalize the secular determinant of Eq. (5).

$$\det|H_{il}(k)-(E+E_{\mathrm{so}})\delta_{il}|=0, \quad (13)$$

where

$$H_{il}(k)=|k+K_{il}|{}^2\delta_{il}+\sum_{m,j} C_{ij}{}^*C_{lm}V(|\mathbf{K}_{ij}-\mathbf{K}_{lm}|)$$
$$+\langle K_i|H_{\mathrm{so}}+V_{\mathrm{so}}|K_l\rangle. \quad (14)$$

So far, we have concerned ourselves with the pseudopotential in general. Actually, the pseudopotential felt by the electrons with s-like symmetry is weaker than that by the other electrons. It is important to realize that, although an s electron sees a stronger relativistic potential, the s repulsive potential is larger than the p

[32] J. C. Slater, Phys. Rev. **36**, 57 (1930).

TABLE II. Fourier transforms of the pseudopotentials for the lead salts.

$\frac{a}{2\pi}\mathbf{k}$	$V^{\mathrm{Pb}}(k)$	$V^{\mathrm{Te}}(k)$	$V^{\mathrm{PbTe}}(k)$	$V^{\mathrm{Pb}}(k)$	$V^{\mathrm{Se}}(k)$	$V^{\mathrm{PbSe}}(k)$	$V^{\mathrm{Pb}}(k)$	$V^{\mathrm{S}}(k)$	$V^{\mathrm{PbS}}(k)$
(111)	−0.1476	−0.1771	0.0925	−0.1499	−0.2073	0.0573	−0.1509	−0.2180	0.0671
(200)	−0.0987	−0.1225	−0.2212	−0.0987	−0.1490	−0.2477	−0.0984	−0.1579	−0.2562
(220)	−0.0287	−0.0429	−0.0716	−0.0260	−0.0624	−0.0885	−0.0242	−0.0686	−0.0928
(113)	−0.0117	−0.0226	0.0109	−0.0088	−0.0395	0.0307	−0.0069	−0.0448	0.0380
(222)	−0.0082	−0.0183	−0.0265	−0.0053	−0.0345	−0.0398	−0.0035	−0.0397	−0.0431
(400)	0.0004	−0.0073	−0.0069	0.0031	−0.0211	−0.0180	0.0047	−0.0258	−0.0210
(133)	0.0037	−0.0027	0.0064	0.0062	−0.0150	0.0211	0.0077	−0.0194	0.0271
(240)	0.0045	−0.0015	0.0030	0.0068	−0.0134	−0.0066	0.0083	−0.0178	−0.0095
(115)	0.0073	0.0034	0.0039	0.0091	−0.0061	0.0152	0.0102	−0.0100	0.0202
(440)	0.0079	0.0049	0.0128	0.0094	−0.0031	0.0062	0.0102	−0.0068	0.0034
(135)	0.0080	0.0055	0.0025	0.0093	−0.0019	0.0111	0.0100	−0.0054	0.0154
(244)	0.0080	0.0056	0.0136	0.0093	−0.0015	0.0077	0.0099	−0.0050	0.0048
(260)	0.0078	0.0060	0.0138	0.0088	−0.0003	0.0085	0.0094	−0.0037	0.0057

one as a consequence of the nonexistence of $1p$ core electrons and of the lower energy of s core levels relative to the p levels. Hence, it is quite improper to assign the same pseudopotential to all electrons. To remedy this point, an excess repulsive potential term V_s is added to the Hamiltonian which acts only on the s component of each valence level. Although a similar statement could be made for p electrons relative to d, it seems to be the case that only s-like levels are highly sensitive to small changes in the crystal potential.[25]

V_s is of the form

$$V_s=-\sum_t(\alpha_t(\varphi_k{}^\alpha,\Phi_{kt}{}^\alpha)E_t\Phi_{kt}{}^\alpha/\varphi_k{}^\alpha), \qquad (15)$$

where the summation is over the outermost s core states only. E_t's are the atomic core state energies.

The matrix elements of V_s to be entered in Eq. (13) are

$$\langle K_j|V_s|K_i\rangle=-\alpha_{\mathrm{Pb}}\langle K_j|\chi_{5s}{}^{\mathrm{Pb}}\rangle\langle\chi_{5s}{}^{\mathrm{Pb}}|K_i\rangle E_{5s}{}^{\mathrm{Pb}}$$
$$-\alpha_{\mathrm{VI}}\langle K_j|\chi_s{}^{\mathrm{VI}}\rangle\langle\chi_s{}^{\mathrm{VI}}|K_i\rangle E_s{}^{\mathrm{VI}}\cos[(\mathbf{K}_i-\mathbf{K}_j)\cdot\boldsymbol{\tau}], \qquad (16)$$

where $\chi_s{}^{\mathrm{VI}}$ is the outermost s Slater atomic core function of the anion. $E_{5s}{}^{\mathrm{Pb}}$ and $E_s{}^{\mathrm{VI}}$ are the energies of the Pb $5s$ and the anion outermost s levels. α_{Pb} and α_{VI} are two more adjustable parameters.

The s-shift effect raises all the s levels relative to the others to a considerable extent, as can be seen from Table VI. If this effect were ignored, the energy bands calculated would be inconsistent with experiment. This s shift is different from the one we reported earlier.[33] Previously, the s shift for each electron was taken to be the sum of two terms each proportional to the amplitude of the square of the wave function on one of the lattice sites. Because of the extreme sensitivity of the bottom of the valence band (states $\Gamma_1(1)$, $L_2'(1)$, and $X_1(1)$ in Table VI) to the s shift, when the parameters α_{Pb} and α_{VI} were chosen to fit energy gaps near the Fermi surface, the s shifts calculated by the former method raised the bottom of the valence band of PbS to somewhere near the Fermi surface. The results we reported previously[33] for PbTe were not nearly so strongly affected by the s shift but did have a somewhat too narrow valence band. The reason the former method does not work well for large s shifts is that it is essentially first-order perturbation theory. When the s shift is included in the potential as it is in our present scheme, the wave functions change in such a manner as to reduce the effect in those levels where it is strongest.

We wish to emphasize that we have only four adjustable band parameters, Z_{Pb}, Z_{VI}, α_{Pb}, α_{VI} plus one spin-orbit (s-o) parameter α. All other parameters are fixed.

The effect of spin-orbit coupling in some semiconductors has been studied by several authors.[34–38] The first quantitative estimation of s-o splitting in Si and Ge was done[38] by treating s-o interaction as a perturbation on the orthogonalized plane wave states. This perturbation calculation is applicable only when the s-o coupling strength is much smaller than the energy gap between any two levels with the same double group symmetry. We know that the valence s-o splitting of the $6p$ electron in a Pb atoms is 0.0936 Ry[39] which is greater than the energy gap 0.013 Ry of PbTe. Consequently, the perturbation approximation can not properly be used. Therefore it is necessary to include the s-o term in the unperturbed Hamiltonian.

We have noticed that the major contribution to the s-o matrix elements comes from the orthogonalization terms within V_{so} in Eq. (7), especially those which are associated with the outermost p and d core functions. We shall only consider this major contribution from the outermost p and d terms. Neglecting the inner core functions will slightly underestimate the valence s-o splitting but the use of the smooth Slater wave functions as

[33] L. Kleinman and P. J. Lin, *Proceedings of the International Conference on the Physics of Semiconductors, Paris, 1964* (Academic Press Inc., New York, 1965), p. 63.

[34] R. J. Elliott, Phys. Rev. **96**, 266, 280 (1954).

[35] L. M. Roth, B. Lax, and S. Zwerdling, Phys. Rev. **114**, 90 (1959).

[36] M. H. Cohen and E. I. Blount, Phil. Mag. **5**, 115 (1960).

[37] M. H. Cohen and L. M. Falicov, Phys. Rev. Letters **5**, 544 (1960).

[38] L. Liu, Phys. Rev. **126**, 1317 (1962).

[39] F. Herman and S. Skillman, *Atomic Structure Calculations* (Prentice-Hall, Inc., Englewood Cliffs, New Jersey, 1963).

TABLE III. Atomic spin-orbit splittings.[a]

Δ_{so} (Ry)		Δ_{so} (Ry)	
S^{3p}	0.0986	Te^{4p}	0.6739
S^{3p}	0.0070	Te^{5p}	0.0618
Se^{3p}	0.4317	Te^{4d}	0.1177
Se^{4p}	0.0307	Pb^{5p}	1.2834
Se^{3d}	0.0721	Pb^{6p}	0.0936
		Pb^{5d}	0.2116

[a] Values are taken from: F. Herman and S. Skillman, *Atomic Structure Calculations* (Prentice-Hall, Inc., Englewood Cliffs, New Jersey, 1963).

the core functions tends to overcompensate this effect. However, all this can be taken into account by introducing an adjustable parameter α into the s-o matrix. We can therefore neglect the term $\langle K_i^\alpha|H_{so}|K_l^\alpha\rangle$ and consider only $\langle K_i^\alpha|V_{so}|K_l^\alpha\rangle$, which we may put into the following form:

$$\langle K_i^\alpha|V_{so}|K_l^\alpha\rangle=-\alpha\sum_t\langle K_i^\alpha|\Phi_{kt}^\alpha\rangle \times\langle\Phi_{kt}^\alpha|K_l^\alpha\rangle\langle\Phi_{kt}^\alpha|H_{so}|\Phi_{kt}^\alpha\rangle, \quad (17)$$

where $\langle K_i^\alpha|$ and Φ_{kt}^α have been defined in Eqs. (2) and (3) and the summation is over the outermost p and d core states of both atoms.

It is convenient to evaluate $\langle K_i^\alpha|\Phi_{kt}^\alpha\rangle$ by expanding a plane wave in terms of spherical Bessel functions.

$$e^{i\mathbf{k}\cdot\mathbf{r}}=4\pi\sum_{l'=0,}^{\infty}\sum_{m'=-l'}^{l'} i^{l'}j_{l'}(kr) \times Y_{l'm'}^*(\Theta,\Phi)Y_{l'm'}(\theta,\varphi), \quad (18)$$

where Θ, Φ are the directional coordinates of $\mathbf{k}$, and θ, φ are those of $\mathbf{r}$.

Let

$$\chi_l^\alpha=(P_l(r)/r)Y_{lm}(\theta\cdot\varphi);$$

then

$$\langle e^{i\mathbf{k}\cdot\mathbf{r}},\chi_l^\alpha\rangle=4\pi i^lY_{lm}^*(\Theta,\Phi)\int rj_l(kr)P_l(r)dr, \quad (19)$$

which can readily be evaluated.

The values of $\langle\Phi_{kt}^\alpha|H_{so}|\Phi_{kt}^\alpha\rangle$ can be obtained from the atomic core s-o splittings listed in Table III. For instance, let $|K_i^\alpha\rangle$ transform like L_3. If the Pb nucleus is taken as the origin then L_3 is d-like about the cation (Pb) and p-like about the anion. The contributions from the $5d$ core state of Pb and the outermost p core state of the anion to

$$\langle\Phi_{kt}^\alpha|H_{so}|\Phi_{kt}^\alpha\rangle$$

are

$$\langle\chi_{5d}^{\alpha\mathrm{Pb}}|H_{so}|\chi_{5d}^{\alpha\mathrm{Pb}}\rangle=(-1/5)\Delta_{5d}^{\mathrm{Pb}}$$

and

$$\langle\chi_p^{\alpha\mathrm{VI}}|H_{so}|\chi_p^{\alpha\mathrm{VI}}\rangle=\tfrac{1}{3}\Delta_p^{\mathrm{VI}},$$

where $\Delta_{5d}^{\mathrm{Pb}}$, Δ_p^{VI} are, respectively, the atomic s-o splittings of the $5d$ core in Pb and the outermost p core in the anion (Te, Se, or S).

If φ_i and φ_j are degenerate in the absence of the s-o interaction, it is convenient to choose them as the eigenfunctions of V_{so}. Therefore we include V_{so} with the pseudopotential in the secular determinant which we diagonalized to determine the coefficients of the plane waves. The case in which the φ_i and φ_j transform like L_3^6 and L_3^{45} is an example. (We have used the notation L_3^6 to represent the irreducible representation being L_3 in single group and L_6 in double group. L_3^{45} refers to the two levels L_3^4 and L_3^5 degenerate by time reversal.) On the other hand, if the φ_i and φ_j are nondegenerate in the absence of the s-o interaction, but belong to the same representation in the double group, such as the representations L_3^6 and L_1^6, we determine first the φ_i and φ_j without considering the offdiagonal elements of V_{so} between them and then diagonalize the matrix $\langle\varphi_i|V_{so}|\varphi_j\rangle$. In doing this, we intermix L_1 and L_3. This kind of mixing plays an important role in determining the effective mass and g factor, as we will discuss in the next two sections.

For points of even lower symmetry, like Σ along the (110) direction, the irreducible representation of the single group are all nondegenerate. Hence we first find the wave functions φ disregarding the spin orbit interaction, since the diagonal terms are zero anyway, and then use these φ's as basis functions to find the eigenfunctions and the eigenvalues of V_{so}.

III. EFFECTIVE MASSES AND g FACTORS OF HOLES AND ELECTRONS

In this section, we shall derive the expressions for the effective masses and g factors of holes and electrons. By analyzing the dependence of the effective masses on the behavior near the band edge we will have some idea about the best choice of the parameters, Z_{Pb}, Z_{VI}, α_{Pb}, and α_{VI}.

It is well known that the dependence of the energy on wave vectors near a symmetry point in the Brillouin zone can be obtained by second-order perturbation theory, i.e.,

$$E_{k_0+k}^\alpha=E_{k_0}^\alpha+\frac{\hbar^2k^2}{2m}+\sum_{\alpha'}\frac{|\langle\psi_{k_0}^\alpha|H'|\psi_{k_0}^{\alpha'}\rangle|^2}{E_{k_0}^{\alpha'}-E_{k_0}^\alpha}+\cdots, \quad (20)$$

where $E_{k_0}^{\alpha'}$, $E_{k_0}^\alpha$, and $E_{k_0+k}^\alpha$ are the energies of the states $\psi_{k_0}^{\alpha'}$, $\psi_{k_0}^\alpha$ and $\psi_{k_0+k}^\alpha$, respectively, and

$$H'=\mathbf{k}\cdot\left(\frac{\hbar\mathbf{p}}{m}+\frac{\hbar^2}{4m^2c^2}\boldsymbol{\sigma}\times\boldsymbol{\nabla}V\right). \quad (21)$$

It has been shown by Pratt and Ferreira[40] that the second term in H' leads to corrections of one part in 10^6 to effective masses calculated from the first term alone. We therefore consider only the first term. The basis functions given in Table IV are chosen for the representations at the point L for a fcc structure.

[40] G. W. Pratt and L. G. Ferreira, *Proceedings of the International Conference on the Physics of Semiconductors, Paris, 1964* (Academic Press Inc., New York, 1965), p. 69.

TABLE IV. Basis functions, selection rules and nonvanishing matrix elements of $H'=\mathbf{k}\cdot\mathbf{p}$ at $L=(\pi/a)(1,1,1)$.

$$L_1^6: \quad \mu_1=\frac{1}{\sqrt{3}}(xy+yz+zx)\downarrow \qquad \mu_2=\frac{1}{\sqrt{3}}(xy+yz+zx)\uparrow$$

$$L_{2'}^{6'}: \quad K_1=\frac{1}{\sqrt{3}}(x+y+z)\downarrow \qquad K_2=\frac{1}{\sqrt{3}}(x+y+z)\uparrow$$

$$L_{3'}^{6'}: \quad \epsilon_1'=(x+\omega y+\omega^2 z)\downarrow \qquad \epsilon_2'=(x+\omega^2 y+\omega z)\uparrow$$

$$L_{3'}^{45'}: \quad \delta_1'=(x+\omega^2 y+\omega z)\downarrow \qquad \delta_2'=(x+\omega y+\omega^2 z)\uparrow$$

$$L_3^6: \quad \epsilon_1=\frac{1}{\sqrt{2}}\{\alpha(z^2+\omega x^2+\omega^2 y^2)\downarrow-\beta(xy+\omega^2 xz+\omega yz)\downarrow\}$$

$$\epsilon_2=\frac{1}{\sqrt{2}}\{\alpha(z^2+\omega^2 x^2+\omega y^2)\uparrow+\beta(xy+\omega xz+\omega^2 yz)\uparrow\}$$

$$L_3^{45}: \quad \delta_1=\frac{1}{\sqrt{2}}\{\alpha(z^2+\omega^2 x^2+\omega y^2)\downarrow-\beta(xy+\omega xz+\omega^2 yz)\downarrow\}$$

$$\delta_2=\frac{1}{\sqrt{2}}\{\alpha(z^2+\omega x+\omega^2 y^2)\uparrow+\beta(xy+\omega^2 xz+\omega yz)\uparrow\}$$

L_i	L_1	L_2'	L_3	L_3'	$L_4^{\pm}$	$L_5^{\pm}$	$L_6^{\pm}$
$L_i\times L_2'$	L_2'	L_1	L_3'	L_3	$L_5^{\mp}$	$L_4^{\mp}$	$L_6^{\mp}$
$L_i\times L_3'$	L_3'	L_3	$L_1'+L_2'+L_3'$	$L_1+L_2+L_3$	$L_6^{\mp}$	$L_6^{\mp}$	$L_4^{\mp}+L_5^{\mp}+L_6^{\mp}$
$L_i\times D_{\frac{1}{2}}$	L_6	L_6	$L_4+L_5+L_6$	$L_4'+L_5'+L_6'$			

Nonvanishing matrix elements

$$\langle\mu_1|H'|K_1\rangle=\tfrac{1}{3}(k_x+k_y+k_z)M_1 \qquad \text{where} \quad M_1=\langle\mu_1|\frac{\partial}{\partial x}+\frac{\partial}{\partial y}+\frac{\partial}{\partial z}|K_1\rangle$$

$$\langle\mu_1|H'|\epsilon_1'\rangle=\tfrac{1}{3}(k_x+\omega k_y+\omega^2 k_z)M_3 \qquad M_3=\langle\mu_1|\frac{\partial}{\partial x}+\omega^2\frac{\partial}{\partial y}+\omega\frac{\partial}{\partial z}|\epsilon_1'\rangle$$

$$\langle\mu_1|H'|\delta_1'\rangle=\tfrac{1}{3}(k_x+\omega^2 k_y+\omega k_z)M_4 \qquad M_4=\langle\mu_1|\frac{\partial}{\partial x}+\omega\frac{\partial}{\partial y}+\omega^2\frac{\partial}{\partial z}|\delta_1'\rangle$$

$$\langle K_1|H'|\epsilon_1\rangle=\tfrac{1}{3}(k_x+\omega k_y+\omega^2 k_z)M_5 \qquad M_5=\langle K_1|\frac{\partial}{\partial x}+\omega^2\frac{\partial}{\partial y}+\omega\frac{\partial}{\partial z}|\epsilon_1\rangle$$

$$\langle K_1|H'|\delta_1\rangle=-\tfrac{1}{3}(k_x+\omega^2 k_y+\omega k_z)M_6 \qquad M_6=\langle K_1|\frac{\partial}{\partial x}+\omega\frac{\partial}{\partial y}+\omega^2\frac{\partial}{\partial z}|\delta_1\rangle$$

$$\langle\epsilon_1|H'|\epsilon_1'\rangle=\tfrac{1}{3}(k_x+k_y+k_z)M_2 \qquad M_2=\langle\epsilon_1|\frac{\partial}{\partial x}+\frac{\partial}{\partial y}+\frac{\partial}{\partial z}|\epsilon_1'\rangle$$

$$\langle\epsilon_1|H'|\delta_1'\rangle=\tfrac{1}{3}(k_x+\omega_{ky}+\omega^2 k_z)M_8 \qquad M_8=\langle\epsilon_1|\frac{\partial}{\partial x}+\omega^2\frac{\partial}{\partial y}+\omega\frac{\partial}{\partial z}|\delta_1'\rangle$$

$$\langle\delta_1|H'|\epsilon_1'\rangle=-\tfrac{1}{3}(k_x+\omega^2 k_y+\omega k_z)M_7 \qquad M_7=\langle\delta_1|\frac{\partial}{\partial x}+\omega\frac{\partial}{\partial y}+\omega^2\frac{\partial}{\partial z}|\epsilon_1'\rangle$$

$$\langle\delta_1|H'|\delta_1'\rangle=-\tfrac{1}{3}(k_x+k_y+k_z)M_9 \qquad M_9=\langle\delta_1|\frac{\partial}{\partial x}+\frac{\partial}{\partial y}+\frac{\partial}{\partial z}|\delta_1'\rangle$$

Matrix elements of the type $\langle\psi_{k_0}{}^{\alpha}|p|\psi_{k_0}{}^{\alpha'}\rangle$ are nonvanishing only when the direct product $\Gamma_\alpha{}^*\times\Gamma_p\times\Gamma_{\alpha'}$ contains the unit representation. Here Γ_p is $L_2'+L_3'$. This condition reduces the number of independent nonvanishing matrix elements. The nonvanishing elements are also listed in Table IV. By using these elements and making the following transformation of coordinates in k space:

$$\begin{aligned} k_1'&=(3)^{-1/2}(k_x+k_y+k_z),\\ k_2'&=(2)^{-1/2}(k_x-k_y),\\ k_3'&=(6)^{-1/2}(-k_x-k_y+2k_z), \end{aligned} \tag{22}$$

we get from (20) the expressions

$$E(L_1^{6\pm})=k_1'^2\left(\frac{\hbar^2}{2m}+\tfrac{1}{3}F_1\right)+(k_2'^2+k_3'^2)\left(\frac{\hbar^2}{2m}+\tfrac{1}{6}F_2+\tfrac{1}{6}F_2'\right),$$

$$E(L_2^{6\pm})=k_1'^2\left(\frac{\hbar^2}{2m}+\tfrac{1}{3}F_3\right)+(k_2'^2+k_3'^2)\left(\frac{\hbar^2}{2m}+\tfrac{1}{6}F_4+\tfrac{1}{6}F_4'\right),$$

$$E(L_3^{6\pm})=k_1'^2\left(\frac{\hbar^2}{2m}+\tfrac{1}{3}F_8\right)+(k_2'^2+k_3'^2)\left(\frac{\hbar^2}{2m}+\tfrac{1}{6}(F_5+F_6+F_7)\right),$$

$$E(L_3^{45\pm})=k_1'^2\left(\frac{\hbar^2}{2m}+\tfrac{1}{3}F_9\right)+(k_2'^2+k_3'^2)\left(\frac{\hbar^2}{2m}+\tfrac{1}{6}(F_{10}+F_{11}+F_{12})\right), \tag{23}$$

where

$$F_1=\sum_j\frac{|\langle\mu_1^{\pm}|\,\partial/\partial x+\partial/\partial y+\partial/\partial z\,|K_{1j}^{\mp}\rangle|^2}{E_0-E_j},$$

$$F_2=\sum_j\frac{|\langle\mu_1^{\pm}|\,\partial/\partial x+\omega^2\partial/\partial y+\omega\partial/\partial z\,|\epsilon_{1j}^{\mp}\rangle|^2}{E_0-E_j},$$

$$F_2'=\sum_j\frac{|\langle\mu_1^{\pm}|\,\partial/\partial x+\omega\partial/\partial y+\omega^2\partial/\partial z\,|\delta_{1j}^{\mp}\rangle|^2}{E_0-E_j},$$

$$F_3=\sum_j\frac{|\langle K_1^{\pm}|\,\partial/\partial x+\partial/\partial y+\partial/\partial z\,|\mu_{1j}^{\mp}\rangle|^2}{E_0-E_j},$$

$$F_4'=\sum_j\frac{|\langle K_1^{\pm}|\,\partial/\partial x+\omega\partial/\partial y+\omega^2\partial/\partial z\,|\delta_{1j}^{\mp}\rangle|^2}{E_0-E_j},$$

$$F_4=\sum_j\frac{|\langle K_1^{\pm}|\,\partial/\partial x+\omega^2\partial/\partial y+\omega\partial/\partial z\,|\epsilon_{1j}^{\mp}\rangle|^2}{E_0-E_j},$$

$$F_5=\sum_j\frac{|\langle\epsilon_1^{\pm}|\,\partial/\partial x+\omega\partial/\partial y+\omega^2\partial/\partial z\,|\mu_{1j}^{\mp}\rangle|^2}{E_0-E_j},$$

$$F_6=\sum_j\frac{|\langle\epsilon_1^{\pm}|\,\partial/\partial x+\omega\partial/\partial y+\omega^2\partial/\partial z\,|K_{1j}^{\mp}\rangle|^2}{E_0-E_j},$$

$$F_7=\sum_j\frac{|\langle\epsilon_1^{\pm}|\,\partial/\partial x+\omega^2\partial/\partial y+\omega\partial/\partial z\,|\delta_{1j}^{\mp}\rangle|^2}{E_0-E_j},$$

$$F_8=\sum_j\frac{|\langle\epsilon_1^{\pm}|\,\partial/\partial x+\partial/\partial y+\partial/\partial z\,|\epsilon_{1j}^{\mp}\rangle|^2}{E_0-E_j},$$

$$F_9=\sum_j\frac{|\langle\delta_1^{\pm}|\,\partial/\partial x+\partial/\partial y+\partial/\partial z\,|\delta_{1j}^{\mp}\rangle|^2}{E_0-E_j},$$

$$F_{10}=\sum_j\frac{|\langle\delta_1^{\pm}|\,\partial/\partial x+\omega^2\partial/\partial y+\omega\partial/\partial z\,|\epsilon_{1j}^{\mp}\rangle|^2}{E_0-E_j},$$

$$F_{11}=\sum_j\frac{|\langle\delta_1^{\pm}|\,\partial/\partial x+\omega\partial/\partial y+\omega^2\partial/\partial z\,|K_{1j}^{\mp}\rangle|^2}{E_0-E_j},$$

$$F_{12}=\sum_j\frac{|\langle\delta_1^{\pm}|\,\partial/\partial x+\omega\partial/\partial y+\omega^2\partial/\partial z\,|\mu_{1j}^{\mp}\rangle|^2}{E_0-E_j}. \tag{24}$$

We have denoted L_1, L_2, L_3 by L_1^+, L_2^+, L_3^+ and L_1', L_2', L_3', by L_1^-, L_2^-, L_3^- for convenience.

We shall see in the next section that the top of the valence band can only be an L_1 state. (See Fig. 1.) The spin-orbit interaction mixes in the nearby L_3 state so that the top of the valence band is the Kramer's doublet $\psi_{\rm val}{}^1=aL_1{}^6\uparrow+bL_{31}{}^6\downarrow$ and $\psi_{\rm val}{}^2=aL_1{}^6\downarrow-bL_{32}{}^6\uparrow$. The bottom of the conduction band may be either of the strongly spin orbit mixed states L_2' or L_3'. Independent of which lies lower in the absence of the s-o interaction we may write the Kramer's doublet for the bottom of the conduction band $\psi_{\rm cond}{}^1=cL_{2'}{}^{6'}\uparrow-dL_{31'}{}^{6'}$ and $\psi_{\rm cond}{}^2=cL_{2'}{}^{6'}\downarrow+dL_{32'}{}^{6'}\uparrow$. Assuming that the other levels are far from the levels under consideration as will be seen to be the case in our problem, the four-level approximation is sufficient for the effective-mass calculations.

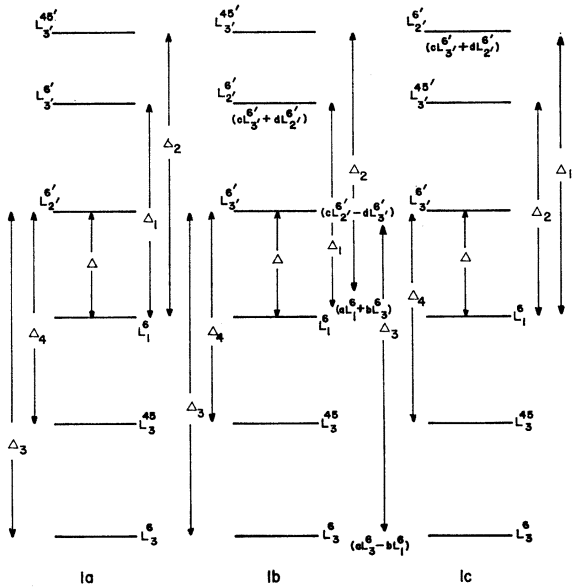

FIG. 1. Three possible orderings of levels around energy gap Δ at $k=(\pi/a)(111)$. Each level is a Kramer's doublet. Thus $aL_3{}^6-bL_1{}^6$ represents $aL_{31}{}^6\downarrow-bL_1{}^6\uparrow$ and $aL_{32}{}^6\uparrow+bL_1{}^6\downarrow$; $aL_1{}^6+bL_3{}^6$ represents $aL_1{}^6\uparrow+bL_{31}{}^6\downarrow$; and $aL_1{}^6\downarrow-bL_{32}{}^6\uparrow$; $cL_{2'}{}^{6'}-dL_{3'}{}^{6'}$ represents $cL_{2'}{}^{6'}\downarrow+dL_{32'}{}^{6'}\uparrow$ and $cL_{2'}{}^{6'}\uparrow-dL_{31'}{}^{6'}\downarrow$; $cL_{3'}{}^{6'}+dL_{2'}{}^{6'}$ represents $cL_{31'}{}^{6'}\downarrow+dL_{2'}{}^{6'}\uparrow$ and $cL_{32'}{}^{6'}\uparrow-dL_{2'}{}^{6'}\downarrow$.

By (23), the components of the effective masses can be put in the following forms.

Holes:

$$\frac{m}{m_t^*}=-1+\frac{4}{3}\left[\frac{|acM_1-bdM_2|^2}{\Delta}+\frac{|adM_1+cbM_2|^2}{\Delta_1}\right],$$

$$\frac{m}{m_t^*}=-1+\frac{4}{6}\left[\frac{|adM_3+bcM_5|^2}{\Delta}+\frac{|acM_3-bdM_5|^2}{\Delta_1}+\frac{|aM_4|^2+|bM_8|^2}{\Delta_2}\right]. \tag{25}$$

Electrons:

$$\frac{m}{m_t^*}=1+\frac{4}{3}\left[\frac{|acM_1-bdM_2|^2}{\Delta}+\frac{|bcM_1+adM_2|^2}{\Delta_3}\right],$$

$$\frac{m}{m_t^*}=1+\frac{4}{6}\left[\frac{|bcM_5+adM_3|^2}{\Delta}+\frac{|acM_5-bdM_3|^2}{\Delta_3}+\frac{|cM_6|^2+|dM_7|^2}{\Delta_4}\right], \tag{26}$$

where the Δ's are indicated in Fig. 1, and the M's are defined in Table IV.

The effect of the wave functions and energy separations of levels on the effective masses is now clear. The matrix elements M depend on the wave functions. The a, b, c, and d are sensitive to small changes of the energy separations.

The first term in the bracket of either of the two equations in (25) is the dominant term because of the smallness of Δ. On the other hand the s-o interaction between L_1^6 and L_3^6 is small. Therefore the top of the valence band is composed mostly of L_1^6; in other words, we expect $a>b$. Judging from the first term in the bracket alone, an increase of d or a decrease of c tends to make the effective mass more anisotropic. As a consequence, the mass anisotropy is larger for the configurations of Figs. 1(b) and 1(c) than for that of Fig. 1(a).

Recently, some reliable experimental work on g factors has been obtained by magneto-optical[2] and Shubnikov–de Haas[12] studies of the lead salts. This information does not play an important role in determining the parameters in our calculations; instead it is used as a supplementary check.

The properties of the g tensor for the conduction electrons or the g value for the paramagnetic impurity ions in a crystal have already been studied extensively by many authors[41–46,35] and need not be repeated here. To describe the g factors of the lead salts, we adopt the $k\cdot p$ approximation. The problem can be somewhat simplified if we consider only the six levels near the band gap. Thus we have derived the following expressions for the g components at the band extrema:

For the valence electrons:

$$g_{\parallel}=2\left\{a^2-b^2-\frac{4}{6}\left[\frac{|bcM_5+adM_3|^2}{\Delta}+\frac{|acM_3-bdM_5|^2}{\Delta_1}-\frac{|aM_4|^2-|bM_8|^2}{\Delta_2}\right]\right\}, \tag{27}$$

$$g_{\perp}=2a^2.$$

For the conduction electrons:

$$g_{\parallel}=2\left\{c^2-d^2+\frac{4}{6}\left[\frac{|bcM_5+adM_3|^2}{\Delta}+\frac{|acM_5-bdM_3|^2}{\Delta_3}+\frac{|cM_6|^2-|dM_7|^2}{\Delta_4}\right]\right\}, \tag{28}$$

$$g_{\perp}=2c^2,$$

where $g_{\parallel}$ is the longitudinal g value along the (111) direction and $g_{\perp}$ is the transverse component.

When the magnetic field $\mathbf{H}$ is at an angle θ with respect to the (111) direction, the effective g value becomes[43]

$$g=\pm(g_{\parallel}^2\cos^2\theta+g_{\perp}^2\sin^2\theta)^{1/2}, \tag{29}$$

with the sign undetermined.

From (27) and (28), it is clear that with such a small Δ in the lead salts, the g factor and hence the Landau level splittings are sure to be large. Because of this, Palik, Mitchell, and Zemel[2] observed the splittings of the $\pi(\Delta_l=0,\ \Delta m_s=0)$ and the $\sigma(\Delta_l=0,\ \Delta m_s=\pm1)$ spectra in magneto-optical experiments. The effective valence and conduction band g factors are determined from the measured splittings of the π lines and the σ lines:

$$\Delta_\pi=|g_v-g_c|\beta_B H,$$
$$\Delta_\sigma=|g_v+g_c|\beta_B H. \tag{30}$$

[41] E. I. Blount, Phys. Rev. **126**, 1636 (1962).
[42] T. Kjeldaas and W. Kohn, Phys. Rev. **105**, 806 (1957).
[43] L. M. Roth, Phys. Rev. **118**, 1534 (1960).
[44] Y. Yafet, Phys. Rev. **106**, 679 (1957).
[45] Y. Yafet, in *Solid State Physics*, edited by F. Seitz and D. Turnbull (Academic Press Inc., New York, 1963), Vol. 14.
[46] C. Kittel, *Quantum Theory of Solids* (John Wiley & Sons, Inc., New York, 1963), p. 281.

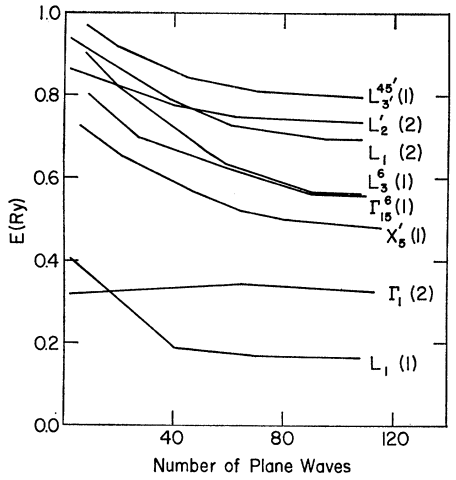

FIG. 2. Convergence of secular determinants for some energy levels in PbS.

IV. ENERGY BANDS

Experimental data on the lead salts indicate that the valence and conduction band extrema are located at $L=(\pi/a)(1,1,1)$ on the Brillouin-zone face.[8] We know that the gap must lie between an adjacent pair of L_1, L_2', L_3, and L_3' levels which are degenerate in the empty lattice. Since L_3^6 transforms like $m_j=\pm\frac{1}{2}$ and L_3^{45} like $m_j=\pm\frac{3}{2}$, it is likely (and calculations confirm) that L_3^{45} lies above the L_3^6 state after the s-o splitting. However, the ordering of L_1^6, $L_{2'}^{6'}$, L_3^{45}, L_3^6, $L_{3'}^{45'}$, and $L_{3'}^{6'}$ levels still cannot be predicted without first knowing the exact potential. Therefore prediction of the ordering will depend mainly on those experimental facts which are directly related to the nature of the conduction and valence band edges and the group theoretical selection rules.

Let us now examine the important experimental information and the theoretical aspects which are helpful in eliminating certain possible orderings.

(a) Symmetry arguments require that all allowed direct optical transitions taking place at L can happen only between states with opposite parity under inversion. The fact that the band edges at L belong to states with opposite parity is confirmed by the observation of Scanlon[47] on the direct band-edge transition.

(b) Relative to the anion Te, Se or S, Pb has a smaller absolute charge and a larger core and hence larger repulsive potential. The unprimed states are anion states and the primed are Pb states in the tight-binding limit. Thus we expect the primed states to lie above the unprimed. This may also be seen by comparing the (11) matrix elements $V_{000}-V_{220}+V_{113}-V_{111}$ of L_3 and $V_{000}-V_{220}-(V_{113}-V_{111})$ of L_3'; the latter is less negative than the former. Hence we suggest that L_3' be above L_3.

[47] W. W. Scanlon, in *Solid State Physics*, edited by F. Seitz and D. Turnbull (Academic Press Inc., New York, 1959), Vol. 9.

TABLE V. Energy gaps (in Ry) in the lead salts. The experimental E_0 values are from Ref. 3; the other experimental values are from reflectivity peaks in Ref. 24.[a]

		Experimental value			Calculated value		
		PbTe	PbSe	PbS	PbTe	PbSe	PbS
E_0	$L_1^6(2)-L_*^{6'}$	0.014	0.012	0.021	0.014	0.012	0.021
E_1	$L_1^6(2)-L_{**}^{6'}$	0.091	0.113	0.136	0.096	0.112	0.130
E_2	$L_3^6(1)-L_{**}^{6'}$	0.180	0.229	0.269	0.185	0.246	0.257
E_3	$\Delta_1^6(3)-\Delta_5^6(2)$	0.257	0.331	0.390	0.264	0.339	0.389
E_4	$\Gamma_1^6(1)-\Gamma_{15}^6(2)$	0.463	0.522	0.596	0.463	0.539	0.599
E_5	$\Gamma_1^6(1)-\Gamma_{15}^8(2)$	0.573	0.669	0.721	0.575	0.659	0.724
E_6	$X_{5'}^{7'}(1)-X_2^7(1)$	0.823	0.919	1.022	0.836	0.971	1.023

[a] $L_*^{6'}=L_{3'}^{6'}(1)$ in PbTe and $L_*^{6'}=L_{2'}^{6'}(2)$ in PbS, PbSe; $L_{**}^{6'}=L_{2'}^{6'}(2)$ in PbTe and $L_{**}^{6'}=L_{3'}^{6'}(1)$ in PbS, PbSe.

(c) The experimental data show that all the effective masses of the lead salts are positive. Hence we know that if L_3' belongs to the conduction band so does L_2', and L_1, L_3 belong to the valence band.

(d) Weinberg and Callaway[48] observed the Knight shift due to the hyperfine interaction between holes and the metal nucleus in PbTe. Their result confirms the fact that the wave function in the valence band edge of the lead salts is s-like at the metal ion site. Therefore we identify the state to be L_1^6. The possibility that it is the L_3^6 state which can have a larger L_1^6 character mixed in by the s-o interaction is dismissed because L_3^{45} must lie above L_3^6.

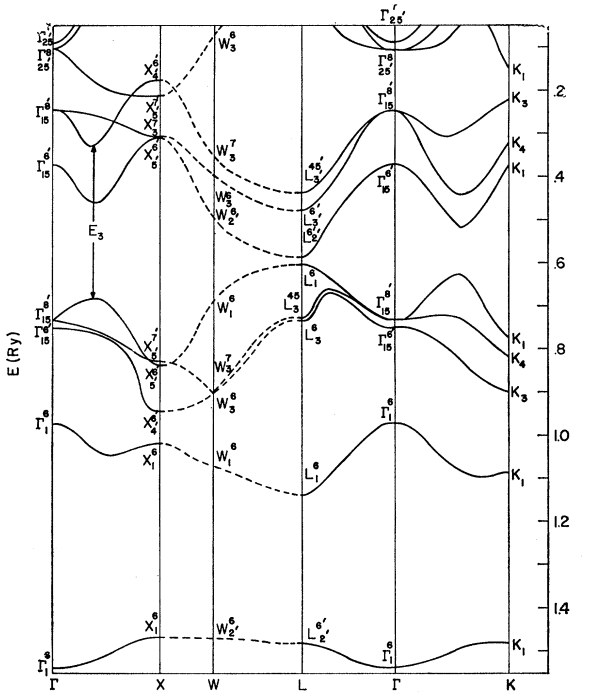

FIG. 3. Energy bands of PbS. The solid lines were calculated at several points. The dashed lines are merely sketched in between symmetry points.

[48] I. Weinberg and J. Callaway, Nuovo Cimento **24**, 190 (1962).

TABLE VI. S shifts for a few s levels in PbTe and PbS.

Level	s shift in PbS(Ry)	s shift in PbTe(Ry)
$\Gamma_1(1)$	1.2186	0.4838
$\Gamma_1(2)$	0.3308	0.3965
$X_1(2)$	0.2332	0.3045
$X_1(1)$	1.3032	0.5659
$L_1(1)$	0.1591	0.2414
$L_1(2)$	0.1013	0.0917
$L_2'(1)$	1.2685	0.5577
$L_2'(2)$	0.1596	0.1024

We conclude from above analysis that the level orderings are limited to the three possibilities shown in Fig. 1. We have already pointed out that due to s-o mixing the bottom of the conduction band in all cases is $\psi_{\text{cond}}=cL_{2'}{}^{6'}-dL_{3'}{}^{6'}$ and that the effective masses become more anisotropic as d gets large and c small. Thus we expect Fig. 1(a) gives the ordering of the L levels in PbS and PbSe and that Fig. 1(b) or 1(c) gives the ordering for PbTe.

The parameters Z_{Pb}, Z_{VI}, α_{Pb}, and α_{VI} were chosen to fit these orderings at L with the correct energy gap E_0 measured[3] at 4°K. In addition the gap at the center of the Brillouin Zone between the $\Gamma_1(2)$ and $\Gamma_{15}(2)$ levels (s and p lead levels in the tight-binding limit) was fit to the optical data of Table V. The spin-orbit parameter α was chosen to fit the splitting of the $\Gamma_{15}(2)$ level (E_5-E_4 in Table V). The splitting in PbTe and PbS is fit with the same value of $\alpha=0.78$. This gives us some confidence in our simplified procedure for calculating spin orbit splittings. The reason for the larger splitting in PbS is that this particular level is a lead level in the tight binding limit. Since PbS is more polar (due to the larger Te repulsive potential) than PbTe, this "lead" level has a larger amplitude on the lead atom in PbS than in PbTe. Since all the energy gaps of PbSe except E_0 lie between those of PbTe and PbS, it is somewhat surprising to find the anomalously large experimental value for the $\Gamma_{15'}(2)$ s-o splitting in PbSe. However, if one examines Cardona's[24] Fig. 1 he will see that the E_4 peak is PbSe is so broad as to practically unobservable. We therefore feel that it is quite likely that the listed experimental value is in error and have chosen the same value for α for all three lead salts. The values chosen for all the parameters are listed in Table I and the Fourier transforms of the potential seen by electrons with no s character are listed in Table II. In Table VI we list some s shifts, i.e., the shift in some energy levels when α_{Pb} and α_{VI} go from zero to the values listed in Table I.

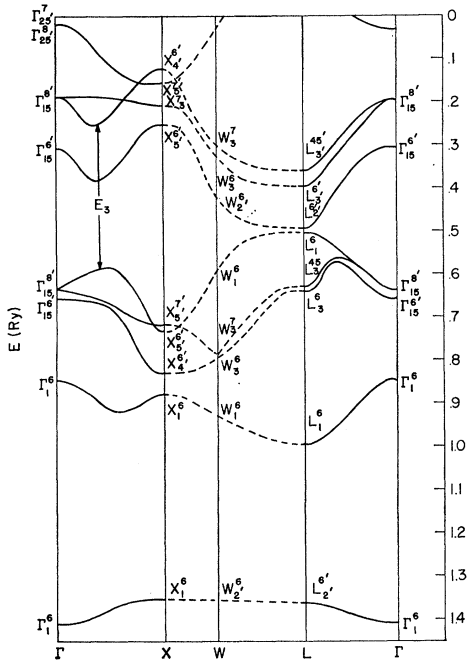

FIG. 4. Energy bands of PbSe. The solid lines were calculated at several points. The dashed lines are merely sketched in between symmetry points.

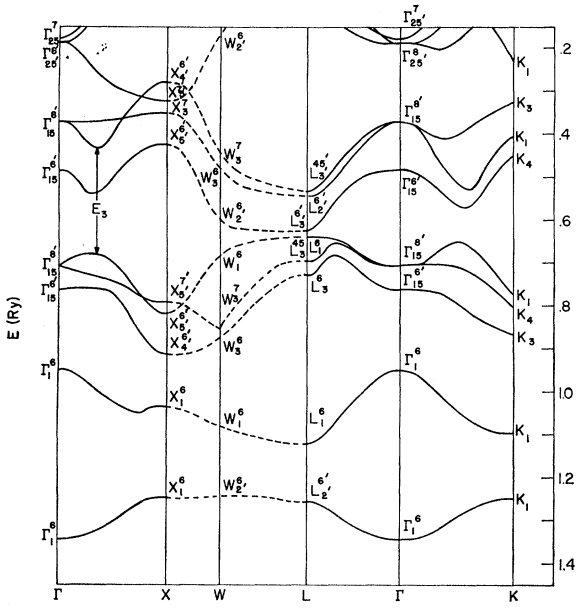

FIG. 5. Energy bands of PbTe. The solid lines were calculated at several points. The dashed lines are merely sketched in between symmetry points.

In our calculation of the energy bands 116 plane waves are included in the expansion of the wave functions which lead to 11th or lower order secular equations at Γ and 35th or lower secular equations along $\Lambda=(k,k,k)$. We have carried out the calculation at the symmetry points Γ, X, L, W, and also at several points along the (1,1,1), (1,0,0) (1,1,0) directions. (The (1,1,0) direction was not calculated for PbSe.) In Fig. 2 is displayed the convergence of several levels for PbS, the most slowly converging case, from which we estimate the lack of convergence after 116 plane waves to be no worse than 0.005 Ry. The calculated energy bands of PbS, PbSe and PbTe are displayed in Figs. 3, 4, and 5. Figure 6 is an enlargement of Fig. 5 showing clearly the

TABLE VII. Comparison of energy difference (in Ry) between anion and cation valence s levels in crystal and free atom.[39]

	PbS	PbSe	PbTe
$\Gamma_1(2)-\Gamma_1(1)$	0.564	0.563	0.393
$E_{\text{val }s}{}^{\text{Pb}}-E_{\text{val }s}{}^{\text{VI}}$	0.641	0.606	0.371

local extrema along the (1,1,0) direction. With a small change in the parameters, the top of the valence band can be made to occur there.

We may compare the energy at which Van Hove singularities in the joint density of states of our calculated energy bands occur with peaks in the reflectivity.[24] The choice is not unique as there occur many more Van Hove singularities than peaks in the reflectivity. The best fit is shown in Table V. All but one of the singularities chosen occur at a symmetry point; E_3 occurs along the (1,0,0) axis and is pointed out in Figs. 3, 4, and 5. The agreement between theory and experiment for twenty of twenty-one gaps is better that 0.02 Ry. The one bad fit, E_6 in PbSe, is for a very badly washed out peak (See Fig. 1 of Ref. 24) and could possibly be due to a misinterpretation of the experimental data. It should be pointed out that no attempt was made to adjust the parameters in the calculation to fit any of the gaps except E_0, E_4, and E_5. On the other hand the agreement between theory and experiment should not be taken too seriously. In the first place one should compare the theoretical joint density of states singularities with peaks in the *derivative* of $\epsilon_2 E^2$ (where ϵ_2 is the imaginary part of the dielectric constant) rather than with peaks in the reflectivity and in the second place the identification of the peaks is not unique; in fact it is not unlikely that a peak in the reflectivity could be due to the interference of two or more nearby singularities in the joint density of states. Therefore we do not claim to have calculated the energy bands with great accuracy but rather to have displayed with reasonable accuracy all the trends as one goes from PbS to PbTe.

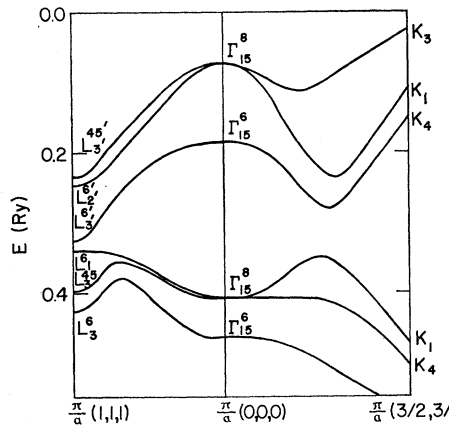

FIG. 6. Enlargement of PbTe bands around forbidden gap.

TABLE VIII. Energy-gap dependence on lattice constant and pressure.

	$\frac{dE_g}{da}$(eV/atomic unit)	$\frac{dE_g}{dP}$(eV cm²/kg)	experimental $\frac{\partial E_g}{\partial P}$
PbS	0.925	-5.44×10^{-6}	-7×10^{-6} [a]
PbTe	0.68	-6.64×10^{-6}	-9×10^{-6} [b]

[a] Reference 22. [b] Reference 15.

Spicer and Lapeyre[49] using photoemission data which unlike optical data give information about energy levels rather than energy gaps, observed a doublet in PbTe due to a pair of levels 0.7 eV and 1.2 eV below the valence band maximum. This doublet disappeared abruptly as the photon energy was increased from 9 to 10 eV. This they attributed to some "last" conduction band level 8.1 to 8.6 eV above the conduction band minimum to which the valence pair could be excited. They assumed (correctly) that these levels were at L. They also determined the existence of a level 2.4 eV below the top of the valence band which they assumed to be elsewhere in the zone. Our calculated PbTe bands have the $L_3{}^{45}(1)$ and $L_3{}^6(1)$ spin orbit split levels lying 0.77 eV and 1.21 eV below the valence band maximum $L_1{}^6(2)$. The $L_{2'}{}^{6'}(3)$ level lies 8.8 eV above the top of the valence band and the transition from L_3 is optically allowed. The level lying elsewhere in the zone could be our $X_{5'}{}^{6'}(1)$ level 2.44 eV below the top of the valence band although it is unclear why the $X_{5'}{}^{7'}$ member of the doublet is not observed. Finally, Spicer and Lapeyre speculated that the optical peak E_1 observed at 1.25 eV might be a pair of unresolved peaks at 1.0 eV and 1.5 eV due to transitions from $L_3{}^{45}(1)$ and $L_3{}^6(1)$ to the bottom of the conduction band $L_{3'}{}^{6'}$. Undoubtedly these contribute to the peak, however we have identified the peak with a third contribution lying between these two in energy. (See Table V.)

Similar studies have been made in PbS by Sacks and Spicer.[50] They find valence-band states approximately 2.0 and 3.0 eV below the valence-band maximum. The 2.0 eV peak they associate with L_3 and place an upper limit of 0.15 eV on its spin-orbit splitting. Our calculated $L_3{}^6(1)$ level lies 1.74 eV below the valence band maximum and is spin orbit split from $L_3{}^{45}(1)$ by 0.067 eV. Our calculated $X_{5'}{}^{7'}(1)$ and $X_{5'}{}^{6'}(1)$ levels lie 2.98 and 3.13 eV below the valence band maximum.

TABLE IX. Calculated values of matrix elements (in Ry) defined in Table IV.

	M_1	M_2	M_3	M_4	M_5	M_6	M_7	M_8
PbTe	0.410	0.306	0.802	0.810	0.779	0.781	0.639	0.674
PbSe	0.464	0.319	0.857	0.866	0.788	0.786	0.678	0.731
PbS	0.467	0.329	0.902	0.901	0.848	0.857	0.717	0.767

[49] W. E. Spicer and G. J. Lapeyre, Phys. Rev. **139**, A565 (1965).
[50] B. H. Sacks and W. E. Spicer, Bull. Am. Phys. Soc. **10**, 598 (1965).

TABLE X. Calculated energy gaps and coefficients of single-group wave functions contained in double-group wave functions.

	a	b	c	d	Δ	$\Delta 1$	$\Delta 2$	$\Delta 3$	$\Delta 4$
PbTe	0.974	0.227	0.668	0.744	0.014	0.096	0.108	0.103	0.071
PbSe	0.999	0.041	0.864	0.504	0.012	0.112	0.148	0.146	0.138
PbS	0.999	0.032	0.881	0.473	0.021	0.129	0.169	0.149	0.144

There are no experimental data on the valence band widths; however, we compare in Table VII the energy difference between $\Gamma_1(1)$ and $\Gamma_1(2)$ which are anion s and Pb s levels in the tight-binding limit with the difference in energy of the two levels in the free atom.[39] The correspondence is striking. In view of the huge s shifts involved (Table VI) it is clear that unlike the diamond family of semiconductors, the lead salts cannot be fit by a momentum-independent pseudopotential. It should be emphasized that the s-shift parameters α were chosen to fit the direct gap and the $\Gamma_1(2)-\Gamma_{15}(2)$ gap, i.e., only the levels $\Gamma_1(2)$, $L_1(2)$, and $L_2'(2)$ were considered in determining the two α's. The shifts of these levels in PbS and PbTe are comparable while the shifts induced in the bottom of the valence band ($\Gamma_1(1)$, $X_1(1)$, $L_2'(1)$ are more than twice as large for PbS as for PbTe. That these huge s shifts, caused by parameters chosen to fit entirely independent data, give reasonable valence band widths, is a consequence of the physical nature of our pseudopotential.

We have calculated the dependence of the energy gap on lattice constant for PbTe and PbS and thus have been able to compare the pressure dependence of the energy gap with the measured value[15,22] in Table VIII. The crystal potential is taken to be a superposition of rigid atomic pseudopotentials when in actual fact the true atomic pseudopotentials are functions of the lattice constant. Thus the agreement between theory and experiment is quite satisfactory and is another indication of the general correctness of our band structure.

The matrix elements defined in Table IV were calculated from the eigenfunctions of our pseudopotential Hamiltonian and are listed in Table IX. The eigenfunctions of the pseudopotential are of course "smooth," i.e., do not contain the rapid oscillations of the true eigenfunctions in the core region. Because the pseudopotential was chosen to fit the eigenvalues, the eigenfunctions are expected to be only approximate; therefore it was felt to be not worthwhile to put in the rapid oscillations by orthogonalizing the smooth functions to the core states. In Table X we list the coefficients of the single group wave functions contained in the double group wave functions as well as the energy gaps needed to calculate the effective masses and g values.

TABLE XI. Comparison of calculated effective masses and g values with experimental values obtained by Cuff, Ellet, Kuglin, and Williams (Ref. 12).

		m_l^{val}	m_l^{cond}	m_t^{val}	m_t^{cond}	g_{11}^{val}	g_{11}^{cond}
PbTe	theory	0.20	0.155	0.037	0.033	−39.51	47.67
	exp	0.31	0.24	0.022	0.024	−51	45
PbSe	theory	0.059	0.054	0.058	0.057	−20.12	21.80
	exp	0.068	0.07	0.034	0.040	−32	27
PbS	theory	0.101	0.086	0.085	0.077	−10.81	10.09
	exp	0.105	0.105	0.075	0.080	−13	12

Using the formulas of the previous section, the effective masses and g values are calculated and compared in Table XI with the experimental values given by Cuff, Ellet, Kuglin, and Williams.[12] Although there is a fair amount of variation in experimental values listed throughout the literature,[1–24] these appear to be typical. The theoretical values are seen to be in reasonably good agreement with the experimental ones. The agreement would be improved if M_2, M_5, and M_3 were somewhat larger and M_1 somewhat smaller. The PbTe matrix elements of Pratt and Ferreira[40] differ from ours in just that way; their matrix elements were calculated from eigenfunctions of a true potential (i.e., not a pseudopotential) and might be expected to be somewhat more accurate than ours. In order to get the correct ordering of levels they were forced to treat the value of their constant "muffin tin" potential between atoms as an adjustable parameter. They used one value of this parameter to obtain the energy gaps and another to obtain the coefficients of the single-group states contained in the double-group wave functions,[51] whereas we obtained all the quantities needed to calculate the effective masses and g values from a single-band calculation whose parameters were chosen to get the right ordering of levels at L but otherwise independently of any effective mass or g-value considerations.

There are no direct experimental determinations of the sign of the g factors. However, Palik, Mitchell, and Zemel[2] have determined from a lack of splitting of the σ line that $g_v \approx -g_c$ in PbS. [See Eq. (30).] They further notice that the σ_l (left handed circular polarization) absorption is greater than the σ_r for the lowest, $l=0$ to $l'=0$, Landau transition. This they attribute to the $m_J'=-\frac{1}{2}$, $l'=0$ conduction states lying below the $m_J'=+\frac{1}{2}$, $l'=0$ conduction states, thus being more fully occupied by free carries and therefore unavailable for the magneto-optical transition. This corresponds to $g_c>0$ and $g_v<0$, in agreement with the theoretical values determined here.

ACKNOWLEDGMENTS

We thank Professor G. W. Pratt for making available to us some of his unpublished effective-mass calculations and Dr. D. C. Mitchell for pointing out a sign mistake in our original g factor calculation.

[51] G. W. Pratt (private communication).